Open access • Journal Article • DOI:10.1109/LAWP.2016.2585308

Four-Element Ultrawideband Textile Cross Array for Dual-Spatial and Dual-Polarization Diversity — Source link

Thijs Castel, Sam Lemey, Patrick Van Torre, Claude Oestges ...+1 more authors

Institutions: Ghent University, Université catholique de Louvain

Published on: 01 Jan 2017 - IEEE Antennas and Wireless Propagation Letters (IEEE)

Topics: Antenna diversity, Diversity gain, Orthogonal frequency-division multiplexing, Bit error rate and Subcarrier

Four-element Ultra-Wideband Textile Cross Array for Dual Spatial and Dual Polarization Diversity

Thijs Castel, Sam Lemey, *Student Member, IEEE,* Patrick Van Torre, Claude Oestges, *Fellow Member, IEEE,* and Hendrik Rogier, *Senior Member, IEEE*

***Abstract*—The emergence of miniaturized flexible electronics enables on-duty first responders to collect biometrical and environmental data through multiple on-body sensors, integrated into their clothing. However, gathering these life-saving data would be useless if they cannot set up reliable, preferable high data rate, wireless communication links between the sensors and a remote base station. Therefore, we have developed a four-element ultra-wideband textile cross array, that combines dual-spatial and dual-polarization diversity, and is easily deployable in a first responder's garment. The impedance bandwidth of the array equals 1.43 GHz, while mutual coupling between its elements remains below -25 dB. For a maximal bit error rate of 1e-4, the array realizes a diversity gain of 24.81dB. When applying Adaptive Subcarrier modulation, the mean throughput per OFDM subcarrier increases by an extra bit/symbol when comparing fourth to second order diversity.**

***Index Terms*—Textile Antenna Array, SIW, Diversity**

I. Introduction

HIGHLY reliable communication in indoor environments is vital for first responders' safety. Indeed, ensuring safe working conditions by remotely monitoring their biometrical and sensor data decreases response time and the number of casualties. Transmit and/or receiver diversity by wearable on-body antenna arrays [1], [2] drastically improves link reliability in Wireless Body Area Networks (WBANs) [3], while wideband systems provide the data rates needed to wirelessly communicate pictures and/or videos. [4] describes Ultra-wideband spatial and polarization diversity for two-element arrays on a rigid substrate. Furthermore, [5] presents a four-element dual-spatial, dual-polarization broadband slot-coupled patch array on an FR-4 substrate, with only 15 dB isolation between the antenna elements, while [6] and [7] describe Substrate-Integrated Waveguide (SIW) cavity-backed arrays with a single feed line, hence, without applying diversity. In [8], 20.8 mm high metamaterial mushrooms walls increase isolation between neighbouring elements in a MIMO antenna system. Yet, this solution is not applicable for low-profile on-body antenna arrays. [9] and [2] propose antenna diversity for off-body communication channels at 2.45 GHz and 60 GHz, respectively. Up to now, receiver diversity in body-to-body scenarios is implemented by several, physically separated on-body antennas [10], [11]. However, avoiding multiple fragile RF cables in a first responder's jacket, by deploying a single antenna array, improves robustness and avoids EMC issues. Moreover, all active transceiver and signal processing electronics may be stacked on a feed plane below its ground plane, yielding a compact active antenna module.

Therefore, we propose a novel ultra-wideband four-element SIW textile antenna array that exploits dual-spatial and dual-polarization diversity and operates in the low duty cycle restricted [3.4-4.8] GHz band [12], while being obtrusively and invisibly integrated into the back section of a first responders jacket. Besides increased reliability through diversity gain, the array realizes additional throughput gain per Orthogonal Frequency Division Multiplexing (OFDM) subcarrier through Adaptive Subcarrier modulation. Moreover, for the first time in literature, the antenna array performance is validated by using it to set up wideband, dynamic SIMO body-to-body links in an indoor office scenario.Section II describes the antenna array design while Section III presents simulation and measurements results, together with the indoor measurement scenario and the calculated bit error rate (BER) characteristics.

II. Antenna array design

Body-worn applications in the public safety segment impose stringent design requirements to textile antennas, which must be unobtrusively integrated into the first responders' outfits, without hindering their movements nor adding weight. Good radiation characteristics and impedance matching are essential, even for a textile antenna in close proximity of the human body. This performance must be maintained when operating in harsh environments, to prevent life-threatening situations. SIW cavity-backed slot (CBS) antennas address these specific design challenges [13]. In this work, the ultra-wideband SIW antenna in [14] serves as the basic building block for the novel four-element antenna array shown in Fig. 1. To obtain high radiation efficiency over an ultra-wide impedance bandwidth, in each antenna element a non-resonant rectangular slot splits the rectangular SIW cavity into subcavities A and B. By careful selection of the cavity and slot dimensions, a 50 Ω grounded coplanar waveguide (GCPW) feed line excites two hybrid modes at neighbouring frequencies. Impedance bandwidth enhancement [15] is obtained by merging both modes.

Fig. 1 shows four of these linearly-polarized UWB SIW CBS antenna elements (AEs), arranged such that the array exhibits fourfold rotational symmetry. Then, subsequent AEs are orthogonally polarized, while equi-polarized AEs (1&3, and 2&4) are separated by a distance of 75.1 mm, being larger than half the wavelength of the smallest operating frequency.

T. Castel, S. Lemey, P. Van Torre, and H. Rogier are with the Department of Information Technology, Ghent University/iMinds, Sint-Pietersnieuwstraat 41, B-9000 Ghent, Belgium (E-mail: thijs.castel@ugent.be)

C. Oestges is with the Institute of Information and Communication Technologies, Electronics and Applied Mathematics, Université Catholique de Louvain, Place du Levant 3, B-1348, Louvain-la-Neuve, Belgium

This work was supported by IAP BESTCOM and UCL

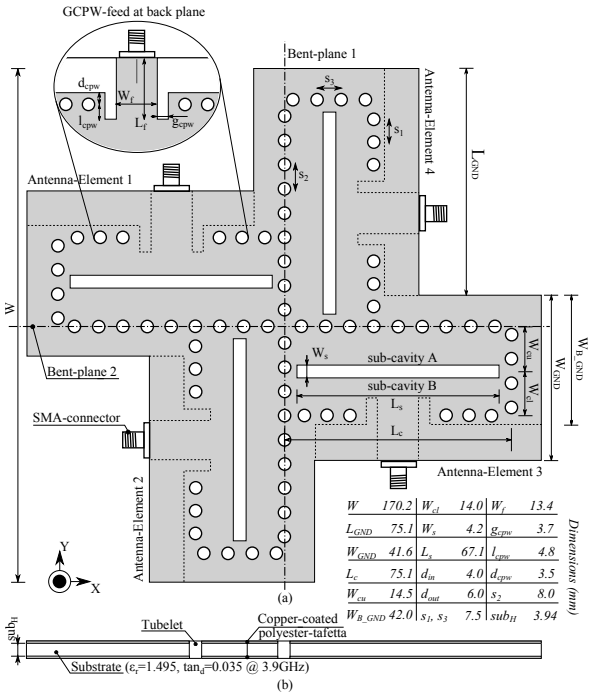

Fig. 1: Four-element textile antenna array. (a) Front view with enlarged inset for the feed section. (b) Cross-section.

In this way, this specific geometry optimally exploits both spatial and polarization diversity by minimizing correlation between receive signals. In addition, cavity sidewalls are shared, while guaranteeing sufficiently low mutual coupling by optimizing the tubelet-spacing s_3 (Fig. 1). A closed-cell expanded-rubber protective foam, typically applied as a protective layer in first responder jackets, is adopted as antenna substrate (ϵ_r=1.495, tanδ=0.035 @ 3.9GHz), whereas the slot and feed layer are implemented in copper-coated Tafetta fabric (surface resistivity 0.18 Ω/sq). Both conductive fabric layers are glued to the substrate by thermally-activated adhesive sheets, after which brass tubular eyelets are inserted to implement the cavities' sidewalls. This specific combination yields a flexible, low-profile and conformal broadband design that facilitates unobtrusive integration. An extensive computer-aided optimization process, carried out in CST Microwave Studio, yields the antenna dimensions (Fig. 1) that provide maximal impedance bandwidth ($|S_{11}|$ < -10 dB w.r.t. 50 Ω) within the-low-duty-cycle restricted [3.4-4.8] GHz band, while keeping mutual coupling between elements below -25 dB.

III. Measurement Results

A. Antenna array performance

First, the array's performance is validated in an anechoic chamber, by measuring its S-parameters from 3.0 GHz to 5.0 GHz (Fig. 2) and its radiation pattern at 3.9 GHz (Fig. 3). Given the fourfold rotational symmetry, Fig. 2 only depicts the array's $|S_{11}|$, as a measure for an element's impedance matching, and its $|S_{21}|$ and $|S_{31}|$, representing the mutual coupling between elements. A very good agreement between simulations and free-space performance is obtained in (2), with a matching to Z_0 = 50 Ω from 3.26 GHz to 4.7 GHz, hence a -10 dB impedance bandwidth of 1.43 GHz, and a very high isolation (> 28.4 dB) between antenna elements.

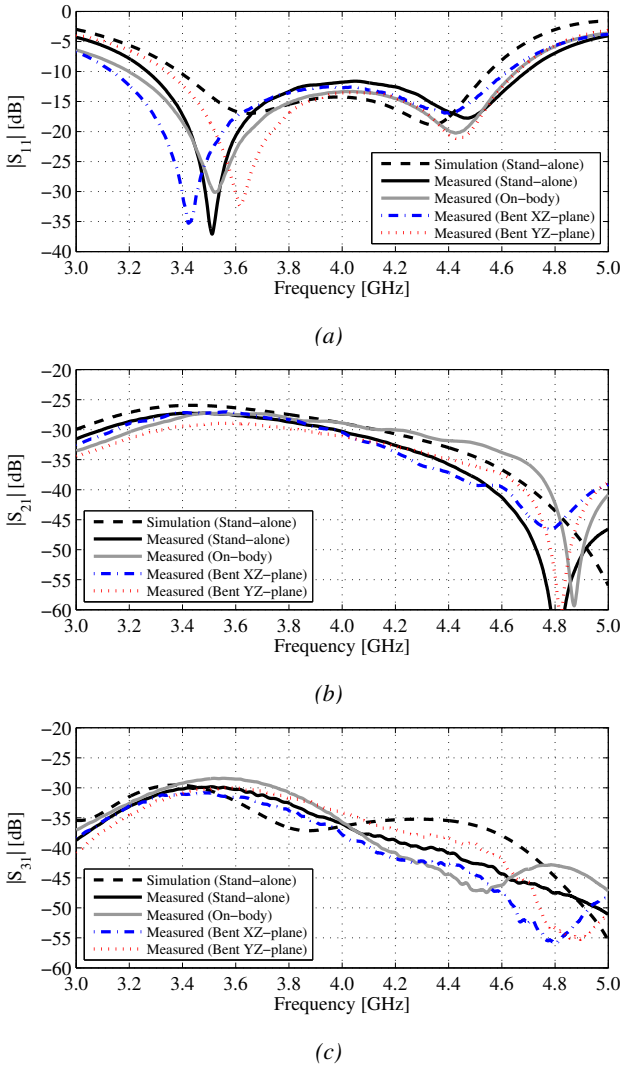

Fig. 2: S-parameters of the four-element antenna array under different conditions. (a) Input impedance matching. (b) Mutual coupling between subsequent antenna elements. (c) Mutual coupling between equipolarized antenna elements.

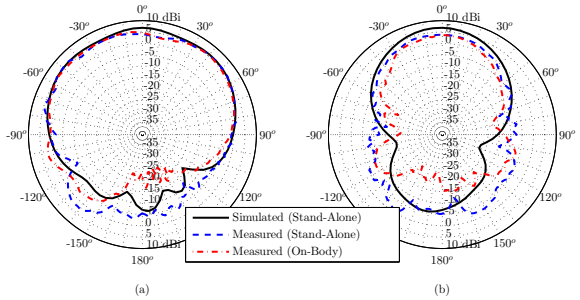

Fig. 3: Measured and simulated standalone radiation pattern together with the on-body radiation pattern in the E-plane (a) and the H-plane (b), at 3.9 GHz

Furthermore, Fig. 3 reveals a stand-alone maximum gain of 4.0 dBi and a front-to-back ratio (FTBR) of 9.6 dB, at 3.9 GHz. In addition, measurements yielded a difference of 12.16 dB between co-polar and cross-polar components along broadside (positive z-direction). Given the fact that the AEs are linearly polarized and that subsequent AEs are orthogonal, providing

fourfold rotational symmetry (Section II), we conclude that subsequent AEs achieve polarization diversity. As the array is worn in close proximity of the human body, its performance was also tested when deployed on the back of a male test person (l=1.79m, w=71kg), as described in Section III-B. Then, Fig. 2 reveals only slight changes in the measured S-parameters, whereas Fig 3 shows a similar maximum gain of 4.6 dBi and an increase in FTBR to 23.6 dB. Finally, the array's S-parameters were also measured when bent with a radius of 14.2 cm along bent-plane 1 and bent-plane 2 (Fig.1), as expected in realistic scenarios. The array maintains its excellent performance under these conditions (Fig.2). Note that, in all considered deployment scenarios, the measured return loss exceeds 5 dB in the complete low duty cycle restricted [3.4-4.8] GHz band. This makes our UWB antenna an ideal candidate to be worn by a first responder. Moreover, the mean effective gain (MEG), calculated for the indoor multipath environment described in [16], equals -2.8 dBi for AEs 1&3 and -3.4 dBi for AEs 2&4, at 3.9 GHz, which indicates good diversity performance.

B. Body-to-Body Measurement Scenario

Wideband body-to-body measurements, replicating real life rescue operations, were performed in an indoor office scenario using the ULB-UCL elektrobit channel sounder with 100 mW TX power, at 3.6 GHz center frequency with 80 MHz useful bandwidth. While the first responder at TX side, equipped with a single SIW textile antenna in the front section of his jacket, scans the hallway, the first responder at RX side, equipped with the novel cross array in the back section of his jacket, scans the offices. There was no Line of Sight (LoS) link between the TX front antenna and the RX cross array at any time, corresponding to a true indoor Non Line of Sight (NLoS) scenario. Measurements were repeated twice for both a vertically and horizontally polarized TX antenna, yielding a total of 60.000 measurement cycles.

C. Correlation Analysis

For further calculations, the frequency-selective wideband channel is subdivided in 256 frequency-flat subcarriers with a bandwidth of 312.5 kHz, as in the 802.11 ac standard [17]. For each of the 256 frequency-flat subcarriers, the complex correlation coefficient ρ between channel samples of two physical channels from the 1×4 SIMO system is calculated. Four separate measurements, each lasting for 197 seconds and gathering 15.000 complex channel samples, are combined. The correlation ρ is calculated based on an array of *60.000 time samples* $\times$ *256 subcarriers* $\times$ *4 SISO links*. Because of the time-varying channel, the complex correlation coefficient is evaluated per subcarrier within a measurement window of 1 s. Since both firefighters walk at 0.5 m/s, the path loss remains constant within this window. Hence, the complex correlation coefficient ρ only comprises body shadowing and small-scale fading. To calculate correlation between, for example, signals from AE1 and AE2, a matrix of 60.000$\times$256 complex correlation coefficients is first time-averaged for each OFDM subcarrier, after the mean value is computed over all 256 subcarriers [18].

TABLE I: Amplitude of the correlation coefficient

	1	2	3	4
1	1	0.41	0.46	0.31
2	0.41	1	0.40	0.31
3	0.46	0.40	1	0.30
4	0.31	0.31	0.30	1

Table I shows that the correlation coefficients remains well below 0.7. Therefore, the four SISO channels are sufficiently decorrelated to ensure that the SIMO-OFDM channel reliability increases when applying receive diversity on subcarrier basis.

D. Bit Error Rate

Let P_k be the transmit power allocated to subcarrier k, σ^2 the noise power and $\mathbf{H}_{i,k}$ the channel matrix of subcarrier k from cycle i. Assume constant TX power with constant power spectral density, while the channel is unknown to the transmitter but perfectly known by the receiver. The Signal-to-Noise Ratio of subcarrier k at cycle i, $\mathrm{SNR}_{i,k}$, is then calculated as $P_k/\sigma^2 \cdot \mathbf{H}_{i,k}\mathbf{H}_{i,k}^H$ for all four SISO links. Furthermore, when applying Maximal Ratio Combining (MRC) per OFDM subcarrier, the subcarrier SNR (during cycle i) is calculated as the sum over $\mathrm{SNR}_{i,k}$ for the corresponding (two or four) AEs. 1×2 *Spatial diversity* combines two equally-polarized AEs, such as AE1&3 or AE2&4 (Fig. 1), whereas 1×2 *polarization diversity* combines two orthogonally-polarized AEs, such as AE1&2, AE2&3, AE3&4 or AE4&1. When applying 1×4 *spatial-polarization diversity*, all four AEs are combined simultaneously. The corresponding BER of subcarrier k at cycle i, for 4-QAM modulation, is calculated as $Q\left(\sqrt{\mathrm{SNR}_{i,k}}\right)$. The mean SNR and mean BER are then found as $1/L \sum_{i=1}^{L} \left(1/N \sum_{k=1}^{N} \mathrm{SNR}_{i,k}\right)$ and $1/L \sum_{i=1}^{L} \left(1/N \sum_{k=1}^{N} \mathrm{BER}_{i,k}\right)$, respectively. The mean SNR is further used to calculate the corresponding E_b/N_0 per RX antenna as $\left(1/N_{RX}\right).\left(1/\log_2 M\right).\overline{\mathrm{SNR}}$ with N_{RX} the number of AEs and M the number of constellation points.

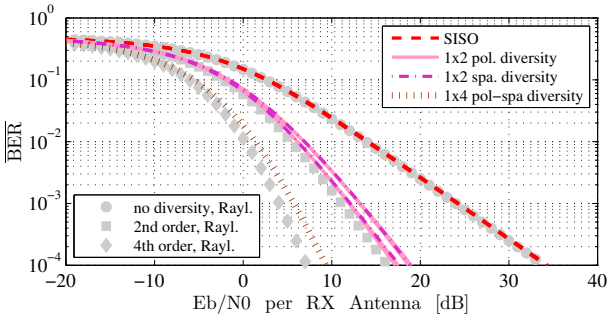

Fig. 4: Measured BER characteristics for uncoded 4-QAM modulation with equal channel gains (after path loss removal)

Fig. 4 shows that 1×4 spatial-polarization diversity is more reliable than 1×2 spatial diversity or 1×2 polarization diversity. For example, for a BER upper limit of 1e-4, the minimal required E_b/N_0 per RX antenna equals 9.36 dB, 17.16 dB, 17.63 dB or even 34.17 dB for 1×4 spatial-polarization, 1×2 polarization, 1×2 spatial and no diversity, respectively. Hence, when applying dual-spatial, dual-polarization diversity for the 1×4 SIMO setup, the required E_b/N_0 per RX antenna is, at least, 24.81 dB lower than for the reference SISO case [19], at the

same maximal BER of 1e-4. Due to additional body shadowing, the channels perform slightly worse than (simulated) Rayleigh fading. Note that the x-axis represents E_b/N_0 per RX antenna, to include both the effects of diversity and array gain.

E. Throughput

When channel state information is available at the transmitter, frequency selectivity can be exploited through Adaptive Subcarrier modulation, which increases the subcarrier throughput for a given BER threshold. For example, for a BER threshold of 1e-4, the subcarrier modulation may be increased from 4-QAM to either 16-, 64- or 256-QAM, compatible with the 802.11ac standard, when E_b/N_0 per subcarrier is larger than 12.19 dB, 16.49 dB or 21.18 dB, respectively. These E_b/N_0-values are obtained from the theoretical BER characteristics for additive white Gaussian noise, since the subcarriers experience frequency-flat fading. The mean throughput is calculated as the mean over N subcarriers and L measurement cycles.

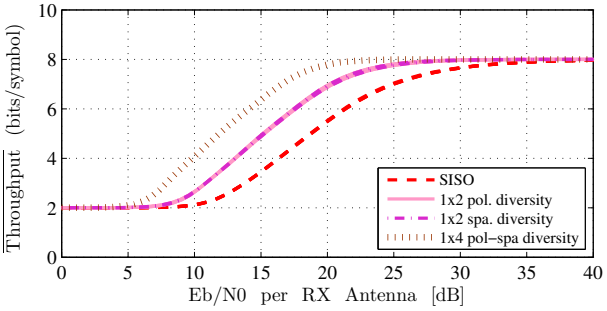

Fig. 5: Measured mean throughput when applying Adaptive Subcarrier Modulation for BER $\leq$ 1e-4 (after path loss removal)

Fig. 5 shows that 1×4 spatial-polarization diversity increases (mean) throughput compared to second-order diversity, when E_b/N_0 per RX antenna is between 5 dB and 30 dB. In this specific range, the modulation order of some subcarriers may be increased for 1×4 spatial-polarization diversity versus 1×2 polarization-, 1×2 spatial- and no diversity. Moreover, when assuming a received E_b/N_0 equal to 10 dB, which is sufficient for reliable timing and frequency offset estimation on each receiver branch, the BER is above 1e-3 for 1×2 spatial or polarization diversity (Fig. 4). However, for 1×4 spatial-polarization diversity, the corresponding BER remains below the pre-set 1e-4 upper BER. This motivates the need for a fourth-order receiver diversity system to guarantee reliable communication at lower E_b/N_0 values. Moreover, by applying Adaptive Subcarrier modulation, an extra bit/symbol can be transmitted for 1×4 spa.-pol. diversity compared to second order diversity, when E_b/N_0 equals 10 dB.

IV. Conclusion

A new, compact four-element textile cross array that exploits dual-spatial and dual-polarization receiver diversity was proposed. 1×4 spatial-polarization diversity guarantees a minimum diversity gain of 24.81 dB, for a maximal BER of 1e-4. Additionally, when comparing fourth- to second order diversity, the mean throughput per subcarrier was increased by an extra bit/symbol through Adaptive Subcarrier modulation. This makes the novel antenna array topology suitable for highly reliable, high-data rate body-to-body communication between first responders in indoor office environments.

References

[1] M. Lucia Scarpello, L. Vallozzi, H. Rogier, and D. Vande Ginste, "High-gain textile antenna array system for off-body communication," *Int. J. Antennas. Propag.*, pp. 1–12, 2012.

[2] N. Chahat, M. Zhadobov, S. Muhammad, L. Le Coq, and R. Sauleau, "60 GHz Textile Antenna Array for Body-Centric Communications," *IEEE Trans. Antennas Propag.*, vol. 61, no. 4, pp. 1816–1824, Apr. 2013.

[3] A. Serra, I. Khan, P. Nepa, G. Manara, and P. Hall, "Dual-polarization and dual-pattern planar antenna for diversity in body-centric communications," in *Int. Symp. AP-S*, Jul. 2008, pp. 1–4.

[4] M. Koohestani, A. Hussain, A. Moreira, and A. Skrivervik, "Diversity gain influenced by polarization and spatial diversity techniques in ultrawideband," *Access, IEEE*, vol. 3, pp. 281–286, 2015.

[5] I. Yeom, H. Kim, J. Jung, and C. W. Jung, "Analysis of spatial/polarization diversity using a broadband slot-coupled patch antenna for the WLAN 802.11A/B/G/N access point," *Microw Opt Techn Let*, vol. 57, no. 5, pp. 1042–1048, 2015.

[6] D.-F. Guan, Z.-P. Qian, Y.-S. Zhang, and Y. Cai, "Novel SIW Cavity-Backed Antenna Array Without Using Individual Feeding Network," *IEEE Antennas Wireless Propag. Lett.*, vol. 13, pp. 423–426, 2014.

[7] R. Bayderkhani, K. Forooraghi, and B. Abbasi-Arand, "Gain-Enhanced SIW Cavity-Backed Slot Antenna with Arbitrary Levels of Inclined Polarization," *IEEE Antennas Wireless Propag. Lett.*, vol. 14, pp. 931–934, 2015.

[8] G. Zhai, Z. N. Chen, and X. Qing, "Enhanced Isolation of a Closely Spaced Four-Element MIMO Antenna System Using Metamaterial Mushroom," *IEEE Trans. Antennas Propag.*, vol. 63, no. 8, pp. 3362–3370, Aug. 2015.

[9] P. Van Torre, M. Lucia Scarpello, L. Vallozzi *et al.*, "Indoor off-body wireless communication: Static beamforming versus space-time coding," *Int. J. Antennas. Propag.*, vol. 2012, no. 3, p. 13, Mar. 2012.

[10] S. Cotton, W. Scanlon, and A. McKernan, "Improving signal reliability in outdoor body-to-body communications using front and back positioned antenna diversity," in *Proc. 6th EUCAP*, Mar. 2012, pp. 3393–3396.

[11] S. Cotton and W. Scanlon, "Channel characterization for single- and multiple-antenna wearable systems used for indoor body-to-body communications," *IEEE Trans. Antennas Propag.*, vol. 57, no. 4, pp. 980–990, Apr. 2009.

[12] "Specific UWB Applications in the bands 3.4-4.8 GHz and 6.8-8.5 GHz Location Tracking Applications for Emergency Services (LAES), Location Tracking Applications Type 2 (LT2) and Location Tracking and Sensor Applications for Automotive and Transportation Environments LTA)," ECC, Tech. Rep., Oct. 2011.

[13] S. Agneessens, S. Lemey, T. Vervust, and H. Rogier, "Wearable, small, and robust: The circular quarter-mode textile antenna," *IEEE Antennas Wireless Propag. Lett.*, vol. 14, pp. 1482–1485, 2015.

[14] S. Lemey and H. Rogier, "SIW textile antennas as a novel technology for UWB RFID tags," in *Proc. RFID-TA*, Tampere, Finland, Sep. 2014, pp. 256–260.

[15] G. Q. Luo, Z. F. Hu, W. J. Li, X. H. Zhang, L. L. Sun, and J. F. Zheng, "Bandwidth-Enhanced Low-Profile Cavity-Backed Slot Antenna by Using Hybrid SIW Cavity Modes," *IEEE Trans. Antennas Propag.*, vol. 60, no. 4, pp. 1698–1704, Apr. 2012.

[16] K. Ogawa and T. Matsuyoshi, "An analysis of the performance of a handset diversity antenna influenced by head, hand, and shoulder effects at 900 MHz: Part I. effective gain characteristics," *IEEE Trans. Veh. Technol*, vol. 50, no. 3, pp. 830–844, May 2001.

[17] "802.11ac," IEEE Standard for Information technology - Telecommunications and information exchange between systems - Local and metropolitan area networks - Specific requirements - Part 11: Wireless LAN MAC and PHY Specifications - Amendment 4: Enhancements for Very High Throughput for Operation in Bands below 6 GHz, Tech. Rep., 2013.

[18] H. Suzuki, T. V. A. Tran, and I. B. Collings, "Characteristics of MIMO-OFDM channels in indoor environments," *EURASIP JWCN*, vol. 2007, no. 1, pp. 1–9, Dec. 2006.

[19] K. Ogawa and J.-i. Takada, "An analysis of the effective performance of a handset diversity antenna influenced by head, hand, and shoulder effectsa proposal for a diversity antenna gain based on a signal bit-error rate and analytical results for the PDC system," *ELECTRON COMM JPN 2*, vol. 84, no. 6, pp. 10–23, 2001.